EFFECTS OF ARTIFICIAL PINS ON THE FLUX PINNING FORCE AND OTHER SUPERCONDUCTING PROPERTIES IN NbTi SUPERCONDUCTORS

K.Matsumoto, Y.Tanaka, *K.Yamafuji, *K.Funaki, *M.Iwakuma, and **T.Matsushita
Yokohama R&D Laboratories, The Furukawa Electric Co.,Ltd.,
2-4-3 Okano, Nishi-ku, Yokohama 220, Japan
*Faculty of Engineering, Kyushu University,
6-10-1 Hakozaki, Higashi-ku, Fukuoka 812, Japan
**Faculty of Computer Science and Systems Engineering,
Kyushu Institute of Technology, 680-4 Kawazu, Iizuka 820, Japan

Abstract--The remarkable enhancement of the global pinning strength in Nb-50wt%Ti alloy was obtained due to introduction of ribbon-shape artificial pins. Simultaneously, however, the depression of B_{c2} was observed. We analyse these behaviors theoretically. The theoretical results explain the experimental results satisfactorily.

I. INTRODUCTION

NbTi superconductors with artificial pins are of considerable interest.[1,2] The hope is that one will be able to design and prepare new materials with superior pinning strengths.

We have already reported the flux pinning characteristics of NbTi composites with aritificial pins. The obtained values of the global pinning force density, F_p, of the island-shape Nb pins were much larger, in the low field range of 1~3T, than those in conventional NbTi composites with α-Ti precipitate pins.[2] On the other hand, the introduction of ribbon-shape Nb pins, instead of the island-shape pins, was much effective for improving the values of F_p in the field range of 3~5T.[3,4] The new technique mentioned here is the most promising method for the enhancement of the pinning strength in NbTi superconductors.

In this paper we present both experimental and theoretical results on the Nb-50wt%Ti system with ribbon-shape artificial pins. The pinning strength and other superconducting properties of the system change according to the variations of size and spacing of pins, or material of pins. The optimized values of critical current density, J_c, in the present series of sepcimens are very high, such as 13900A/mm^2 at 2T and 3780A/mm^2 at 5T.

II. EXPERIMENTAL

The superconducting wires studied were multifilamentary composites containing Nb-50wt%Ti filaments with artificial pins. We prepared three kinds of specimens of A, B and C, with different pins. The designed specifications of specimens are shown in Tab.1, where d_f is the diameter of NbTi filaments, d_p, d_w, and d_s are the thickness, the width, and the spacing of artificial pins in the transverse cross section, and the wave length $\Lambda = d_p+d_s$. An example of the cross section, before final drawing, of artificial pins embedded in NbTi filament is also shown in Fig.1. The volume fraction of artificial pins in specimen A is highest, and specimens B and C have the similar ones. The shape of each pin is a thin ribbon such as that of α-Ti precipitates in practical NbTi wires.

Firstly, in fabrication proccess of specimens, the elementary composite rods assembled with Nb plates and NbTi plates were prepared for specimens A and B. For specimen C, we used a Nb/Ti/Nb triple-layered plate, instead of a Nb plates, where the volume ratio of Nb to Ti is 6.8. For each specimen, the about 900 elementary rods were inserted into a Cu tube, and the resulting ingot was hot extruded, drawn down, and cut into 55 rods. These rods were again inserted into a Cu tube, and the tube was extruded and cold drawn down to the appropriate sizes of Λ's for superconductivity measurements.

Superconductivity measurements were made for estimat-

Manuscript received August 24, 1992

Table 1 Specifications of artificial pins in the specimens. Λ is the wave length, $\Lambda=d_p+d_s$.

Specimen	Material of pins	d_f	d_w	d_s	d_p
A	Nb	281.3Λ	11.25Λ	0.66Λ	0.34Λ
B	Nb	409.1Λ	15.00Λ	0.71Λ	0.29Λ
C	Nb+Ti	391.3Λ	11.74Λ	0.72Λ	0.28Λ

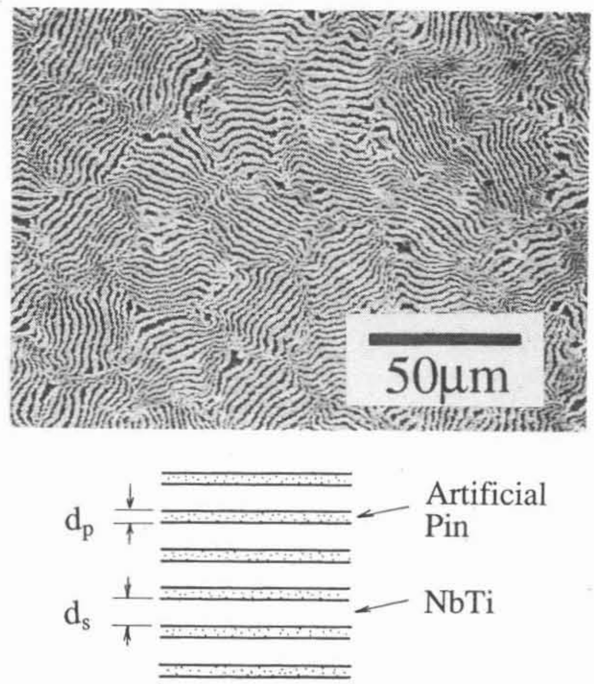

Fig.1 SEM photogragh of the cross section, before final drawing, of artificial pins embedded in a NbTi filament, where the dark layers are NbTi layers and the bright layers are Nb layers. The lower figure is the schematic cross sectional view of the artificial pins/NbTi composite layers.

1051-8223/93$03.00 © 1993 IEEE

ing T_c, B_{c2}, and J_c of each specimen obtained.[4] T_c was defined by the magnetization measurement. B_{c2} was determined by the resistive method with the small constant current density of 0.1A/mm^2. The values of J_c, per cross sectional area including artificial pins, were measured at 4.2K by ususal four probe method with the criterion of $10^{-14}\Omega$m.

III. RESULTS

T_c in the present specimens did not change remarkably from those of the constituent elements, (Nb: T_c~9.2K, Nb-50wt%Ti: T_c~9.0K),[5] with decreasing Λ. For example, the observed T_c's of specimen A with Λ=84.5nm, specimen B with Λ=59.2nm, and specimen C with Λ=51.4nm are 9.01K, 9.09K, and 9.14K, respectively.

On the other hand, as shown in Fig.2, the observed B_{c2}'s showed large decreases with decreasing Λ from about 11T which is the value of B_{c2} for single phase Nb-50wt%Ti alloy. Finally, the measured B_{c2} for specimen A with the highest pinning volume fraction seems to approach about 9T, and that for specimen B with smaller pinning volume fraction closes to about 9.5T, as shown in Fig.2. However, the depression of B_{c2} in sepcimen C is slighter, even though the volume fraction of pins is the same as that in specimen B.

Figure 3 shows the dependence of J_c values for each specimen on the magnetic field, B. The high J_c values of each specimen were obtained below Λ=100nm. In specimen A, the J_c values were high in the low field range of 1~3T, such as 13900A/mm^2 at 2T and 8360A/mm^2 at 3T when Λ=94.1nm, while the J_c values in specimen B were optimized in the middle field range of 3~5T when Λ=51nm. These values were, for example, 7800A/mm^2 at 3T and 3780A/mm^2 at 5T. But, these superior J_c properties in specimens A and B were depressed consideraby in higher field region. The high field J_c properies were improved only in specimen C. The relatively higher value of 840A/mm^2 at 8T, compared with those of artificial pins hitherto reported, was attained when Λ=25.8nm.

The magnetic field dependence of F_p for each specimen is shown in Fig.4. The maximum F_p value was about 28GN/m^3 and this value was obtained for specimen A with Λ=94.1nm. In specimen B, the maximum F_p value was about 24GN/m^3 when the field was 3T and Λ=51nm. In specimen C, however, the maximum F_p value was about 14GN/m^3 at 4T andΛ=63.2nm, although its optimum magnetic field shifted to higher field side.

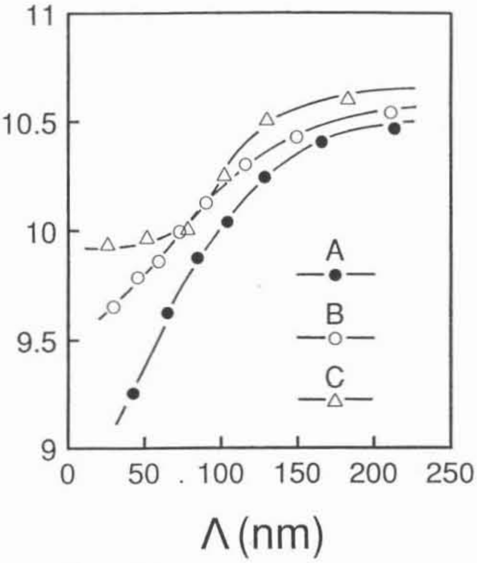

Fig.2 The variations of the observed B_{c2} values of specimens A, B, and C with decreasing Λ.

The maximum value and the position of the peak F_p can be changed noteworthily, as presented here, by the selections of the pinning structures and the material of artificial pins. However, the saturation-like tendencies, where the F_p value is independent of the increase of pin density, were observed above 7T for speceimens A and B. But, the F_p versus the magnetic field curves in specimen C showed a nonsaturation tendency even in the high field region near B_{c2}.

IV. DISCUSSION

A. Upper Critical Field

Firstly, let us consider the mechanism of a large decrease of B_{c2}, which is one of the serious causes for the depression

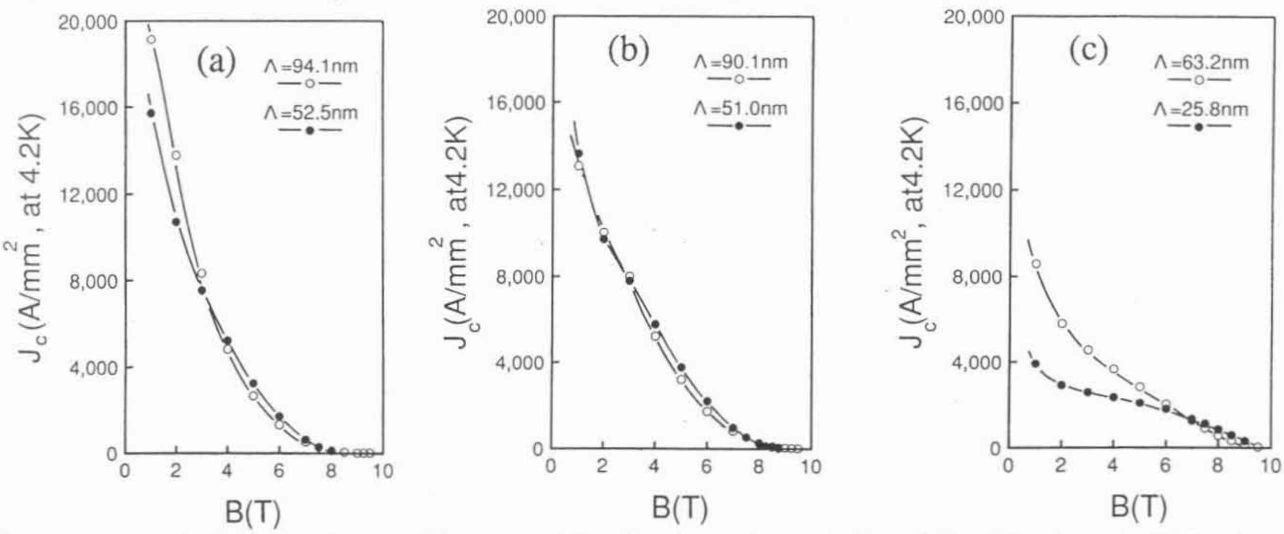

Fig.3 The magnetic field dependences of the observed J_c values in specimens A, B, and C. (a) Specimen A, (b) Specimen B, (c) Specimen C. (Λ=d_s+d_p)

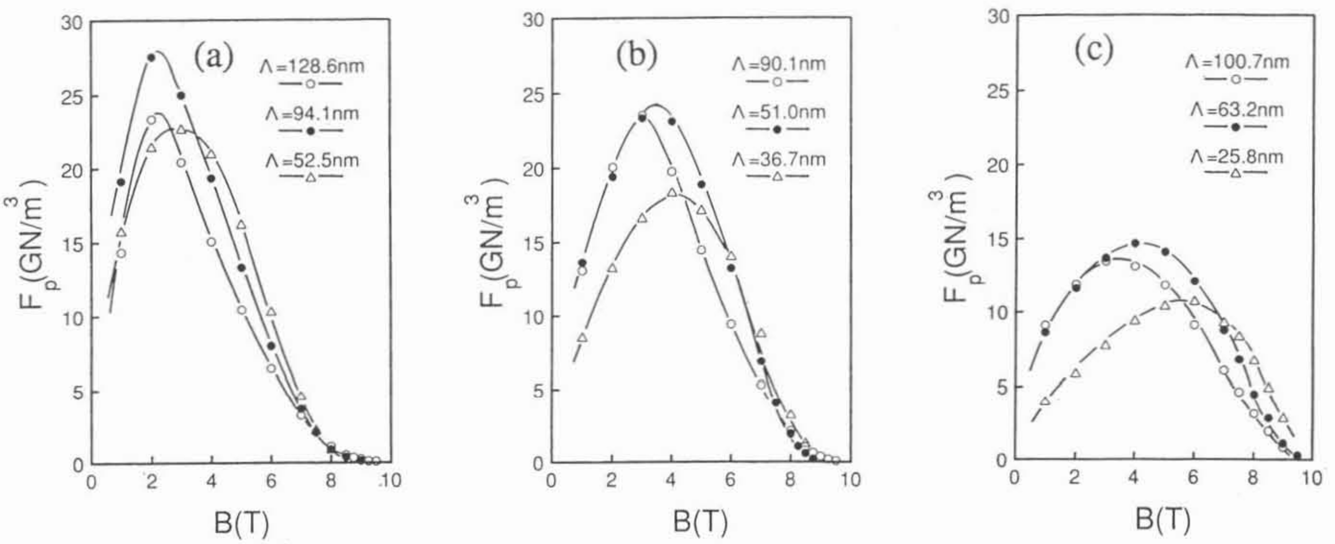

Fig.4 The magnetic field dependences of the observed F_p values in specimens A, B, and C. (a) Sepcimen A, (b) Specimen B, (c) Specimen C. ($\Lambda=d_s+d_p$)

of pinning properties in high fields.

The microstructure in present specimens with artificial pins can be approximated by ramdomly distributed multilayered clusters which are composed of thin artificial pin layers and NbTi layers. Generally, multilayered superconductors have an anisotropic property of B_{c2}, where $B_{c2//}$, the upper critical field parallel to the layer, is the highest one and $B_{c2\perp}$, the upper critical field perpendicular to the layer, is the lowest one.[6] The observed B_{c2}, in present specimens, by means of resistive method is determined by the clusters whose flat layer surface is parallel to the direction of magnetic field.

If Λ is much smaller than the coherence length of artificil pin layer, each NbTi layer couples strongly through artificial pin layer due to the proximity effect. Then, the system behaves as an effective homogeneous material and $B_{c2\perp}$ in the perpendicular field direction can be expressed as

$$B_{c2\perp} = \phi_0/2\pi\xi_{eff}^2, \quad (1)$$

where ϕ_0 is the flux quantum and ξ_{eff} is the effective coherence length of the system. We assume ξ_{eff} is given by

$$\xi_{eff}=\{(d_s/\xi_s^2+d_p/\xi_p^2)/\Lambda\}^{-1/2}, \quad (2)$$

where ξ_s and ξ_p are the coherence lengths of a NbTi layer and an artificial pin layer. Figure 5 shows the model of the nucleation of superconductivity expressed by ξ_{eff} in the multilayer.

On the other hand, as shown in Fig.5, the nucleation in this limit occurs extending to several layers when the magnetic field is applied parallel to the layer. Assuming that the size of nucleus is expressed by both ξ_s in parallel direction of the layer and ξ_{eff} in perpendicular direction of the layer, we have the following expression as

$$B_{c2//}=\phi_0/2\pi\xi_s\xi_{eff}. \quad (3)$$

We can calculate the values of B_{c2} in strongly coupled limit using Eqs.(1), (2), and (3). The values of $B_{c2\perp}$ of specimens A and B are 7.4T and 7.9T, respectively, assuming ξ_s=5.5nm with B_{c2}=11.0T as NbTi layers and ξ_p=28.7nm with B_{c2}=0.4T as Nb layers.[5] Then we have 9.0T and 9.3T as the values of $B_{c2//}$ for specimens A and B, respectively. For specimen C, we must estimate, first of all, the B_{c2} value of the Nb/Ti/Nb composite triple-layer. In strongly coupled limit, the compostie layer can be expected to have about 3T as the final B_{c2} value, since the volume ratio of Nb to Ti is 6.8 and this corresponds to Nb-7wt%Ti as an uniform alloy.[7] Using this value, we have $B_{c2\perp}$ =8.9T and $B_{c2//}$=9.8T for specimen C. The observed final B_{c2} values of specimens A, B and C in the above limit, predicted from the experimental results in Fig.2, are ~9T, ~9.5T, and ~9.9T, respectively. The calculated $B_{c2//}$ values agree with the experimental results very well. This means simple Eqs.(1),(2), and (3) are available for estimating the final B_{c2} value in the present composite system.

B. Global Pinning Force

The maximum F_p value of 28GN/m^3 was obtained in specimen A, and the peak position of F_p is very low field of 2T. This behavior is similar to that of island-shape Nb pins, although the maximum F_p value of specimen A is 1.4 times higher than that of island pins. In addition, specimen B also has the very high F_p values of 24GN/m^3 at 3T and 19GN/m^3

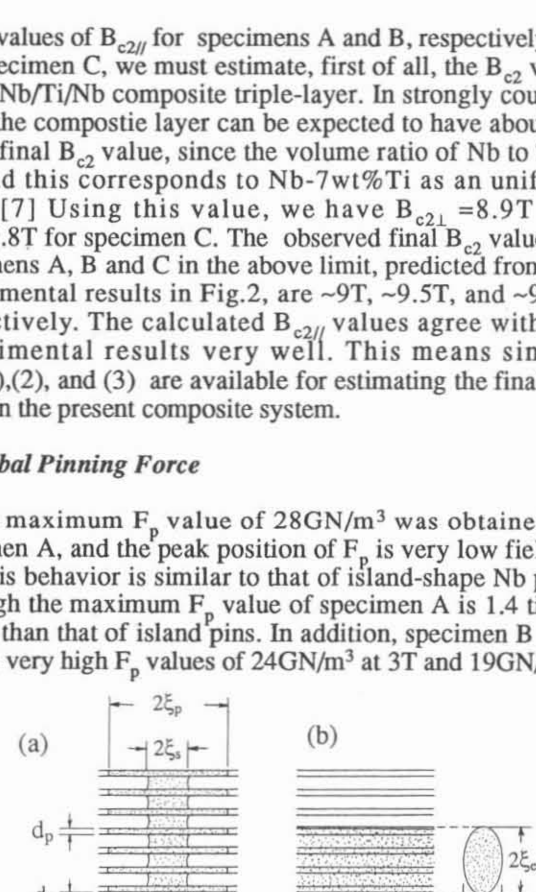

Fig.5 Sketch of the nucleus of superconductivity in the artificial pin/NbTi multilayers in different field directions: (a) perpendicular to the layer, (b) parallel to the layer.

at 5T. The present specimens have very large F_p value compared with the conventional NbTi wires, so that their strong pinning mechanism is particularly interseting for understanding how to raise the F_p values.

Generally, as the elementary pinning force, f_p, becomes strong, the pinning efficiency approaches unity. In this limit, F_p is given by the linear sum,[4]

$$F_p \cong f_p N_p, \tag{4}$$

where N_p is the pin density. When an artificial pin is in the normal state, its f_p value may be roughly described by

$$f_p(b;\theta) \cong (B_{c2}^2/4\mu_0\kappa^2\xi)V(1-b), \tag{5}$$

where B_{c2}, ξ, and κ are the upper critical field, the coherence length, and GL parameter, of the composite system, μ_0 is a permeability in vacuum and $b=B/B_{c2}$. V is the overlapping volume between artificial pin and the core of interacting fluxoid, depending on the angle θ between the flat surface of artificial pin and the fluxoid. This value is maximum at $\theta=0$ and minimum at $\theta=\pi/2$, and is expressed when $d_p \geq 2\xi$ as,

$$V(\theta)=\pi\xi^2 d_w \quad ; \theta=0,$$
$$=\pi\xi^2 d_p \quad ; \theta=\pi/2. \tag{6}$$

If the interface of artificial pin/NbTi is effective pinning center, we can assume the effective number of N_p as

$$N_p \cong 1/(d_w \Lambda a_f), \tag{7}$$

where a_f is the fluxoid spacing.

Both the maximum and minimum F_p values of the local cluster composed of atificial pin layers and NbTi layers can be estimated based on Eqs.(4),(5),(6),and(7). For example, the calculated maximum and minimum F_p values for specimen A with Λ=94.1nm are 103GN/m^3 at $\theta=0$ and 2T and 3GN/m^3 at $\theta=\pi/2$ and 2T, respectively, using $\kappa\cong30$ and the measured B_{c2} of 9.98T. In calculation, we assumed that the values of $B_{c2//}$ and $B_{c2\perp}$ are the same because Λ is larger than ξ_p. In the same way, the maximum and minimum F_p values for specimen B with Λ=51.0nm are 187GN/m^3 and 3.6GN/m^3 at 3T, using $\kappa\cong30$ and the measured B_{c2} of 9.84T. The observed F_p values of specimens are the averaged values of them, because the artificial pin/NbTi clusters are distributed randomly in each NbTi filament. Actually, the peak F_p values of specimens A and B, obtained experimentally, are 28GN/m^3 and 24GN/m^3, and their efficiencies for the calculated maximum F_p values are 27% and 13%, respectively. The difference between two efficiencies may be attributed to the difference of the designed pinning structure.

Next, we consider the F_p values of specimen C. Its maximum F_p value is much smaller than that of specimen B, though the volume fraction of two specimens are very similar. However, the high field properties of specimen C are superior to those of specimens A and B. These characteristics are due to the introduction of the Nb/Ti/Nb layer, instead of the Nb layer.

The improvements of high field properties may be attributed to the smaller depression of B_{c2} due to the proximity effect, compared with specimens A and B, while the decrease of the observed F_p value may be explained as follows. The superconducting properties of the Nb/Ti/Nb layer approach those of Nb-7wt%Ti alloy and the B_{c2} value of the system becomes about 3T, in the strongly coupled limit. In this case, the difference of B_{c2} between the Nb/Ti/Nb layer and the NbTi layer may be regarded as the origin of the elementary pinning force, if the T_c values of two layers are nearly the same. Then, we assume the following expression of f_p, when B<3T,

$$f_p(b) \cong f_{p0}\{1-(\xi_p^2|\psi_p|^2/\xi_s^2|\psi_s|^2)\}, \tag{8}$$

where f_{p0} is the elementary pinning force when Ti layer is absent, s and p denote the NbTi layer and the Nb/Ti/Nb layer, and ψ is the superconducting order parameter perturbed by the proximity effect. We assume, for simplicity, $|\psi_p|^2 \cong (1-B/B_{c2p})$ and $|\psi_s|^2 \cong (1-B/B_{c2s})$.

According to Eq.(8), the calculated maximum F_p value at 2T, of specimen C with Λ=63.2nm, is about 70GN/m^3 at $\theta=0$ using $\kappa\cong30$ and the measured B_{c2} of 10.0T. The calculated value is much smaller than that of specimen B without Ti layer. This is the main reason for the decrease of the maximum F_p of sepcimen C. The observed F_p value of about 11GN/m^3 at 2T is 16% of the calculated value.

V. SUMMARY

The remarkable enhancements of J_c were observed in Nb-50wt%Ti superconductors with artificial pins. These values are much larger than those in the conventional NbTi wires in the magnetic field range below 5T. We could also explain theoretically both the depression of B_{c2} in the system with the artificial pins using the effective coherence length, and the properties of F_p based on the linear sum.

ACKNOWLEDGMENT

We would like to thank H.Takewaki of the Furukawa Electric Co.,Ltd. for his helpful cooperation.

REFERENCES

[1] L.R.Motowidlo, H.C.Kanithi, and B.A.Zaitlin, "NbTi superconductors with artificial pinning structures", Adv.Cryog.Eng., vol.36A, pp.311-316, 1990.

[2] K.Yamafuji, N.Harada, Y.Mawatari, K.Funaki, T.Matsushita, K.Matsumoto, O.Miura, and Y.Tanaka, "Achievement of high current density in NbTi superconducting multifilamentary wires by introducing designed artificial pins", Cryogenics, pp.431-438, June 1991.

[3] K.Matsumoto, Y.Tanaka, K.Yamafuji, K.Funaki, M.Iwakuma, and T.Matsushita, "Flux pinning properties in NbTi superconducting wires with artificial pins", in the Proc. of 7th US-Japan Workshop, Fukuoka, Japan, Oct.1991, pp.153-157.

[4] K.Matsumoto, Y.Tanaka, K.Yamafuji, K.Funaki, M.Iwakuma, and T.Matsushita, to be published.

[5] C.Meingast, P.J.Lee, and D.C.Larbalestier, "Quantitative description of a high J_c NbTi superconductor during its final optimization strain:I. Microstructure, T_c, H_{c2}, and resistivity", J.Appl.Phys., vol.66, pp.5962-5970.

[6] Y.Obi, M.Ikebe, Y.Muto, and H.Fujimori, "Upper critical fields of NbTi based multilayered materials", Jpn.J.Appl.Phys., supplement vol. 26-3, pp.1445-1446, 1987.

[7] Y.J.Qian, J.Q.Zheng, Bimal K.Sarma, H.Q.Yang, J.B.Ketterson, and J.E.Hilliard, "Critical-field measurements in NbTi composition-modulated alloys", J.Low Temp.Phys., vol.49, pp.279-294, 1982.